

Real-time optical control of $\text{Ga}_{1-x}\text{In}_x\text{P}$ film growth by p -polarized reflectance

N. Dietz^{a)} and V. Woods

Department of Physics, North Carolina State University, Raleigh, North Carolina 27695

K. Ito and I. Lauko

Center for Research in Scientific Computation, North Carolina State University, Raleigh, North Carolina 27695

(Received 4 November 1998; accepted 1 February 1999)

The engineering of advanced optoelectronic integrated circuits implies the stringent control of thickness and composition. These demands led to the development of surface-sensitive real-time optical sensors that are able to move the control point close to the point where the growth occurs, which in a chemical beam epitaxy process is the surface reaction layer, built up of physisorbed and chemisorbed precursor fragments between the ambient and film interface. In this context, we explored the application of p -polarized reflectance spectroscopy (PRS) for real-time monitoring and control of pulsed chemical beam epitaxy during low-temperature growth of epitaxial $\text{Ga}_{1-x}\text{In}_x\text{P}$ heterostructures on Si(001) substrates. A reduced order surface kinetics model has been developed to describe the decomposition and growth kinetics of the involved organometallic precursors and their incorporation in the film deposition. We demonstrate the linkage of the PRS response towards the surface reaction chemistry, composition, film growth rate, and film properties. Mathematical control algorithms are applied that link the PR signals to the growth process control parameters to control the composition and growth rate of epitaxial $\text{Ga}_{1-x}\text{In}_x\text{P}$ heterostructures. © 1999 American Vacuum Society. [S0734-2101(99)08004-5]

I. INTRODUCTION

Applying optical probe techniques to real-time characterization of thin-film growth inherits the challenge of relating surface chemistry processes that drive the growth process to growth/film properties, such as composition, instantaneous growth rate, or structural layer quality. The need is especially acute for chemical deposition methods, where the surface plays a major role in the growth process and the addition of small amounts of new reactants (e.g., dopants) can severely modify growth chemistries.^{1,2} The limited knowledge in these areas slowed the progress in understanding and controlling thin-film growth. To improve the understanding of the driving mechanisms of growth processes, nonintrusive real-time techniques have been developed, focusing on the monitoring of surface processes by reflection high-energy electron diffraction (RHEED),³ reflectance difference spectroscopy (RDS),⁴ surface photoabsorption (SPA),⁵⁻⁷ and p -polarized reflectance spectroscopy (PRS).⁸⁻¹⁰

Presently, the only two techniques that combine the advantage of high surface sensitivity with bulk film properties characterization are (a) an integrated spectral ellipsometry (SE)/RDS spectrometer developed by Aspnes *et al.*¹¹ and (b) PRS.⁸⁻¹⁰ Both techniques aim to integrate the optical response to surface processes with the optical response to bulk properties to monitor and control the deposition process with submonolayer resolution.

This contribution describes the recent developments utilizing p -polarized reflectance spectroscopy for closed-loop deposition control during pulsed chemical beam epitaxy

(PCBE) of III-V heteroepitaxial growth. The demonstrated high sensitivity of PRS towards surface reactions processes in the context of real-time monitoring of PCBE has opened new possibilities for characterization and control of thin-film deposition processes. During heteroepitaxial $\text{GaP}/\text{Ga}_x\text{In}_{1-x}\text{P}$ growth on Si under PCBE conditions the surface is periodically exposed to metalorganic precursors, which causes a periodic in composition and thickness altered surface reaction layer (SRL). The control of a growth process using the optical signature from the SRL that feeds the underlying growth requires detailed instantaneous simulation and prediction of the surface chemistry and its link to the optical properties of the outermost layer in a multilayer medium. A reduced order surface kinetics (ROSK) model has been developed that describes the growth process with a mathematically reduced number of surface reaction equations using heteroepitaxial $\text{Ga}_x\text{In}_{1-x}\text{P}$ growth as an example. The dynamic in the molar concentrations of the surface constituent evolution gives information on the SRL thickness, its optical response in a four-media-layer approximation, the instantaneous growth rate, and the composition of the growing film. For real-time closed-loop deposition control, a virtual substrate approach was used, an approach recently introduced by Aspnes for product-driven deposition control.¹²

II. EXPERIMENTAL SETUP AND RESULTS

For monitoring both the bulk and surface properties during heteroepitaxial $\text{Ga}_x\text{In}_{1-x}\text{P}$ growth on Si, p -polarized reflectance spectroscopy has been integrated in a pulsed chemical beam epitaxy system, as schematically shown in Fig. 1(b). In PCBE, the surface of the substrate is exposed to

^{a)}Corresponding author; electronic mail: ndietz@unity.ncsu.edu

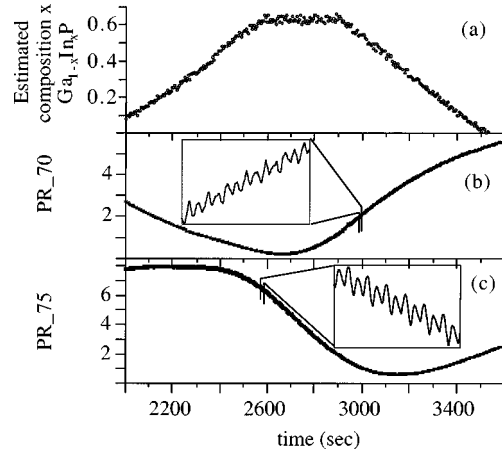
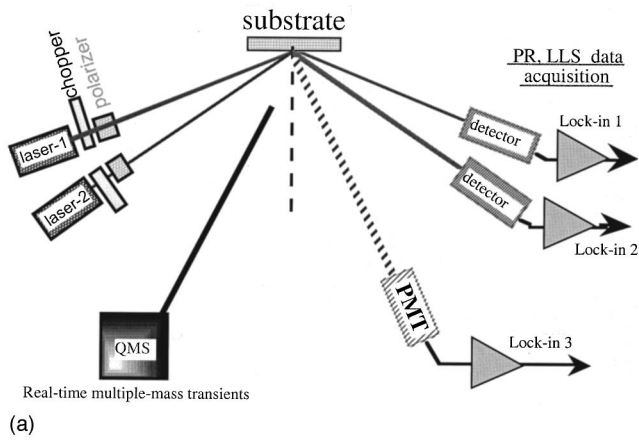


FIG. 3. Growth of a graded $\text{Ga}_{1-x}\text{In}_x\text{P}$ layer (see the graded $\text{Ga}_{1-x}\text{In}_x\text{P}$ region marked in Fig. 2): (a) estimated composition, determined via *ex situ* x-ray diffraction analysis. (b) and (c): evolution of the PR signals. The insets show the fine-structure response at two different positions with different TMI:TEG flow ratios and different PR responses to it. The ROSK model introduced below will demonstrate how the optical PR response is linked to composition and growth rate.

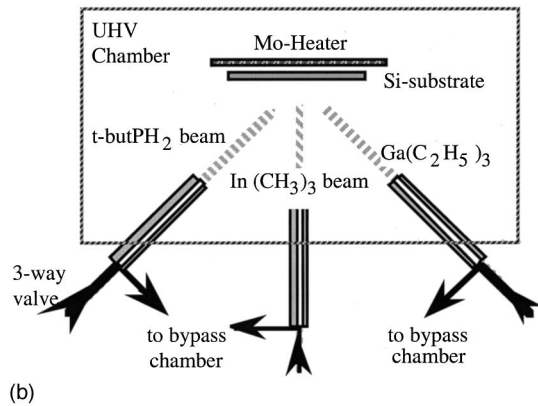


FIG. 1. (a) Schematic setup of PRS, LLS, and quadrupole mass spectroscopy (QMS) for real-time growth characterization. (b) Setup of pulsed chemical vapor deposition system for epitaxial III-V compound semiconductor growth.

pulsed ballistic beams of $(\text{C}_4\text{H}_9)\text{PH}_2$ (TBP) and $\text{Ga}(\text{C}_2\text{H}_5)_3$ (TEG) and $\text{In}(\text{CH}_3)_3$ (TMI) at, typically, 350–450 °C to accomplish nucleation and overgrowth of the silicon by an epitaxial $\text{GaP}/\text{Ga}_{1-x}\text{In}_x\text{P}$ film. For PRS and laser light scattering (LLS), we employed *p*-polarized light beams (λ_1

$=632.8$ nm and $\lambda_2 = 650$ nm) and Glan–Thompson prisms, as illustrated in Fig. 1(a). The beams impinge on the substrate at two angles of incidence PR70 ($\varphi = 71.5^\circ$) and PR75 ($\varphi = 75.2^\circ$). The LLS intensity is detected using a photomultiplier tube (PMT). Further details on the experimental conditions are given in previous publications.^{8–10,13–23}

Figure 2 shows the evolution of the PR signals during growth of $\text{Ga}_{1-x}\text{In}_x\text{P}/\text{GaP}$ on $\text{Si}(001)$ at 420 °C, recorded for PR70 and PR75 at $\lambda = 650 \pm 5$ nm and at $\lambda = 632.8$ nm, respectively. The growth process is composed of four sections: (a) substrate and surface preconditioning; (b) deposition of a GaP buffer layer lattice matched to the substrate; (c) growth of a graded $\text{Ga}_{1-x}\text{In}_x\text{P}$ layer, which is shown in more detail in Fig. 3; and (d) growth of a GaP cap layer.

During the preconditioning period, the PR signals change

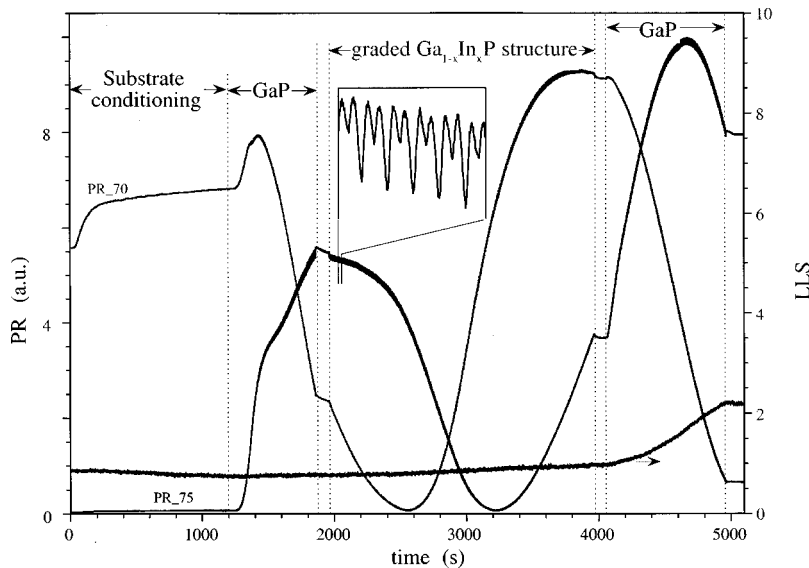
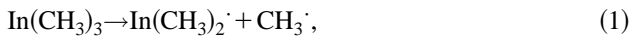


FIG. 2. Growth monitored by PRS during heteroepitaxial $\text{Ga}_{1-x}\text{In}_x\text{P}/\text{GaP}$ on $\text{Si}(001)$.

according to the temperature dependency of the substrate. The signals are used to verify independent temperature measurements and to calibrate the actual surface temperature. After initiating growth, minima and maxima are observed in the time evolution of the PR signals due to the interference phenomena as the film grows. Please note that both signals are phase shifted, which is due to the fact that one angle of incidence (PR75) is above—and the other (PR70) below—the pseudo-Brewster angle of the growing film material. This angle is defined for an infinitive thick layer only and is in the range between 71° and 74° for Ga_{1-x}In_xP monitored at 632.8 nm. Superimposed on the interference oscillations of the reflected intensity is a fine structure that is strongly correlated to the time sequence of the supply of precursors employed during the steady-state growth conditions.

III. REDUCED ORDER SURFACE KINETICS (ROSK) MODEL FOR Ga_{1-x}In_xP DEPOSITION

The reduced order surface kinetics model for the binary compound semiconductor GaP growth from triethylgallium and tertiary-butylphosphine TBP has been discussed previously.²³ At this, we extend this model by adding the decomposition mechanism for trimethylindium for the description of heteroepitaxial Ga_xIn_{1-x}P growth. The TMI de-fragmentation and sufficient retention of fragments on the surface occurs within a limited process window in the temperature range 700 K < T < 850 K for Si(100).²⁴ The kinetics of TMI pyrolysis for the growth of Ga_xIn_{1-x}P utilizing trimethylindium, triethylgallium, and tertiary-butylphosphine as source vapors has been discussed in detail elsewhere.^{20,25} Its progression can be summarized in three consecutive steps:



where the vertical dashes and superscript dots denote lone electron pairs and single valence electrons, respectively.

For GaP growth on Si(100), we have shown that the decomposition of TBP is fast and elimination of ethyl radicals from the TEG fragments represents the rate limiting step.²⁶ Depending on the delay between the TEG and TBP source vapor pulses, carry over of TEG fragments from one precursor pulse cycle to the next may occur, which establishes in steady state a surface reaction layer consisting of a mixture of reactants and products of the chemical reactions that drive the epitaxial growth process. In a realistic model, the SRL represents a multicomponent mixed phase with a variety of radical reactions that have to be added to the above reactions (1)–(3) and to the reaction products from the TEG and TBP decomposition.²⁶ The thickness and composition of the SRL depends on the relative heights and widths of the employed TMI, TEG, and TBP source vapor pulses and their repetition rate. We note that some of the intermediate fragments of the source vapor molecules in the SRL that feed III–V CBE may carry permanent dipole moments, which are likely to contrib-

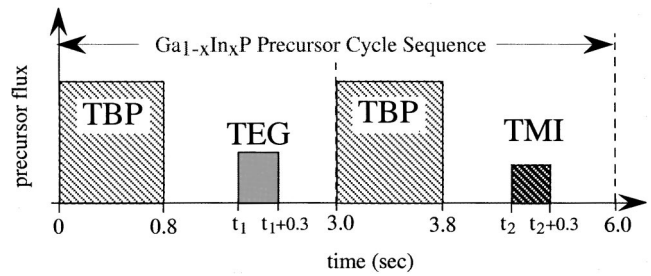


Fig. 4. Schematic representation of a precursor cycle sequence used for the growth of the ternary compound semiconductor Ga_{1-x}In_xP grown via the organometallic precursors TBP, TEG, and TMI. The start positions for TEG and TMI, indicated by t_1 and t_2 , were 1.5 and 4.5 s for the experiment shown in Fig. 2.

ute to the stabilization of the SRL. In view of intermolecular interactions, deviations of the SRL from ideal behavior can be expected. However, the objective here is to relate the measured PR signals to the dynamic of the decomposition processes of the SRL constituents, and to relate the kinetics of growth and real-time modeling for closed-loop process control.

The reduced order kinetic model for the compound semiconductor Ga_{1-x}In_xP summarizes all chemical reactions in one dominant bimolecular reaction for the TBP pyrolysis (first precursor, PC1), two dominant bimolecular reactions for the TEG decomposition (second precursor, PC2), and two dominant reactions for the TMI decomposition process. All precursors are supplied sequentially separated by pauses as shown schematically in Fig. 4.

With the above-mentioned assumptions, the differential rate equations for the molar concentrations n_i of the SRL constituents in the Ga_{1-x}In_xP system can be written as

$$\frac{d}{dt} n_1(t) = n_{\text{TBP}} - \tilde{a}_1 n_1(t) - \tilde{a}_4 n_3(t) n_1(t) - \tilde{a}_7 n_6(t) n_1(t), \quad (4)$$

$$\frac{d}{dt} n_2(t) = n_{\text{TEG}} - \tilde{a}_2 n_2(t), \quad (5)$$

$$\frac{d}{dt} n_3(t) = \tilde{a}_2 n_2(t) - \tilde{a}_3 n_3(t) - \tilde{a}_4 n_3(t) n_1(t), \quad (6)$$

$$\frac{d}{dt} n_5(t) = n_{\text{TMI}} - \tilde{a}_5 n_5(t), \quad (7)$$

$$\frac{d}{dt} n_6(t) = \tilde{a}_5 n_5(t) - \tilde{a}_6 n_6(t) - \tilde{a}_7 n_6(t) n_1(t), \quad (8)$$

with the two incorporation reactions

$$\frac{d}{dt} n_4(t) = \tilde{a}_4 n_3(t) n_1(t), \quad (9)$$

$$\frac{d}{dt} n_7(t) = \tilde{a}_7 n_6(t) n_1(t), \quad (10)$$

for GaP and InP, respectively.

Equations (4)–(6) describe the reduced order TBP and TEG pyrolysis as described earlier.²³ n_{TBP} and n_{TEG} denotes periodic supply functions expressed in terms of the molar concentration of TBP and TEG reaching the surface. To this, we add Eqs. (7) and (8) that describe the parametrized reduced order TMI pyrolysis. This pyrolysis is assumed to be similar to the TEG pyrolysis that is described by a two-step decomposition process using two generalized reaction parameters \bar{a}_5 and \bar{a}_6 with a periodically supplied molar concentration n_{TMI} of TMI. The formation of GaP and InP and its incorporation in the underlying film is summarized in the reactions Eqs. (9) and (10). The composition x for the compound semiconductor Ga_{1-x}In_xP is expressed as the averaged ratio of molar concentration over a cycle sequence

$$x = \frac{\int \frac{d}{dt} n_7}{\int \left(\frac{d}{dt} n_4 + \frac{d}{dt} n_7 \right)} dt, \quad (11)$$

and the instant film growth rate g_{fl} is given by

$$g_{fl} = \frac{1}{A} \left[\bar{V}_{\text{GaP}} \frac{d}{dt} n_4 + \bar{V}_{\text{InP}} \frac{d}{dt} n_7 \right]. \quad (12)$$

At this point, the SRL is treated as a homogeneous ideal solution and the surface area A is assumed to be constant for simplicity. Also note that the surface structure, number of reaction sides, and inhomogeneous reactions are not explicitly addressed at this point and are integrated into the reaction parameters \bar{a}_4 and \bar{a}_7 .

The temporal thickness evolution of the SRL is given by

$$d_1(t) = \frac{1}{A} [n_1 \bar{V}_1 + n_2 \bar{V}_2 + n_3 \bar{V}_3 + n_5 \bar{V}_5 + n_6 \bar{V}_6], \quad (13)$$

where \bar{V}_i are the molar volumes of the constituents in the SRL.

Based on the above reaction chemistry, we model the linkage between the measured PR signals and the surface kinetics on the basis of a reduced order surface kinetics model and a four-media stack: ambient/SRL/epilayer/substrate, which represents the simplest possible description of the optical response under the conditions of the PCBE processes. For the interpretation of the time dependence of the four-media stack reflectance $R_4(t)$ in terms of the chemical kinetics in the SRL that drives epitaxial growth, the dielectric function of the SRL, ϵ_1 , must be linked to its composition. Such a linkage can be established by approximating the dielectric function of the SRL through an effective dielectric function ϵ_1 , parametrized and expressed as the sum over all molar fractions x_i contributing to the SRL:

$$\epsilon_i(\omega) = \epsilon_\infty + \sum_{i \neq 4,7} x_i(t) F_i(\omega) \quad \text{and} \quad x_i(t) = \frac{n_i(t)}{\sum_k n_k(t)}. \quad (14)$$

The dielectric function of the SRL is obtained by summing over the contributions of all its constituents, identified by the label i . In Eq. (14), $F_i(\omega)$ denotes optical response

factors associated with transitions that characterize specific molecular fragments, and ω denotes the frequency at which ϵ_1 is evaluated.

This ROSK model provides a description of how to relate changes in composition and thickness of the SRL to an effective dielectric function $\epsilon_1(\omega, t)$ and $d_1(t)$, respectively. It allows also to obtain the instantaneous composition x and growth rate $g_{fl}(t)$ of the Ga_xIn_{1-x}P film. The ROSK data are incorporated in Fresnel's equation that determines the reflectance amplitude rr of the p -polarized light as follows: Consider the four-layer media composed of ambient/SRL/film/substrate. We model the reflection/refraction of the surface reaction layer by an effective medium with the homogeneous dielectric function $\epsilon_1(t)$ and the thickness $d_1(t)$. Let us denote the four media by the indices $n=0,1,2,3$ labeled from the ambient to the substrate. The reflection coefficient $r_{n-1,n}$ from the $(n-1)$ st media to n th media is given by

$$r_{n-1,n} = \frac{\epsilon_n \sqrt{\epsilon_{n-1} - \epsilon_0 \sin^2 \varphi} - \epsilon_{n-1} \sqrt{\epsilon_n - \epsilon_0 \sin^2 \varphi}}{\epsilon_n \sqrt{\epsilon_{n-1} - \epsilon_0 \sin^2 \varphi} + \epsilon_{n-1} \sqrt{\epsilon_n - \epsilon_0 \sin^2 \varphi}}, \quad (15)$$

where ϵ_n is the complex dielectric function of the n th media. The factor Φ_n for the n th media is given by

$$\Phi_n = \frac{2\pi d_n}{\lambda} \sqrt{\epsilon_n - \epsilon_0 \sin^2 \varphi}, \quad (16)$$

where d_n is the thickness of the n th media. For the formulation of the control problem we analyze the multilayer film stack of Ga_xIr_{1-x}P with different composition x using the virtual interface (VI) method described by Aspnes.^{27–29} Consider the above-formulated four-layer media composed of ambient/SRL/film/substrate and replace it through a four-media stack that is built up by

- (i) the ambient (0);
- (ii) the surface reaction layer represented by Eq. (1);
- (iii) a the near-surface layer (u) describing the growing film with composition x ; and
- (iv) a virtual substrate (v), represented by its complex virtual reflectance coefficients r_v .

With this, the total reflectance amplitude is given as

$$rr_4 = \frac{r_{01} + \hat{r} e^{-2i\Phi_1}}{1 + r_{01} \hat{r} e^{-2i\Phi_1}} \quad \text{with} \quad \hat{r} = \frac{r_{1u} + r_v e^{-2i\Phi_u}}{1 + r_{1u} r_v e^{-2i\Phi_u}}. \quad (17)$$

Here, r_{01} , r_{1u} , and Φ_1 are functions in $\epsilon_1(t)$ and $d_1(t)$. The virtual reflectance coefficient r_v can be determined by knowing the thicknesses and dielectric constants for each of the underlying layers. However, even under exact knowledge of each of these parameters, the recursive formula that determines r_v can be numerically unstable and nonrobust.

At this point, we can establish a mathematical control loop, as schematically outlined in Fig. 5, for the control of the deposition process with a control of composition x in the Ga_xIn_{1-x}P surface layer, utilizing the real-time measured PR signals at the two different angles of incidence φ_i , $i=1,2$:

$$R_i(t) = |rr_4|^2 = h_i(\epsilon_1(t), d_1(t), gr(t), x(t)) + \text{noise}, \quad (18)$$

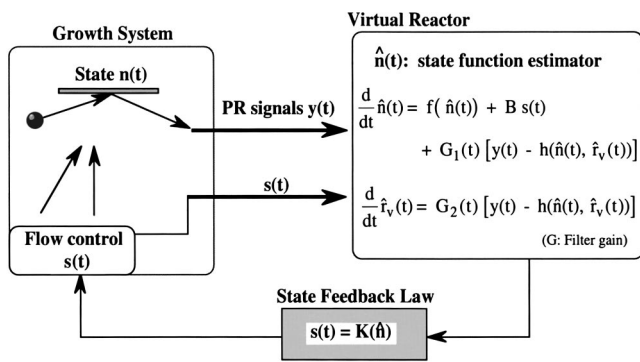


FIG. 5. Control of heteroepitaxial Ga_{1-x}In_xP growth: the compensator design consists of three elements: (1) the ROSK model described by f ; (2) filter gains $G_i(t)$ based on nonlinear-filtering techniques; and (3) feedback law \mathbf{K} based on dynamical programming.

where the output functions h_i are determined by Eqs. (15)–(18). The nonlinear filtering algorithms applied for real-time estimates³⁰ yield the composition x , the growth rate $gr(t)$, and the dielectric function of the surface layer.

Now, we can formulate the problem of controlling the growth rate and composition of Ga_xIn_{1-x}P as

$$\text{Min} \int_{t_0}^T \left\{ c_1 \left| \frac{x_d(t)}{1-x_d(t)} - \frac{\int_{t_0}^t \frac{d}{dt} n_7}{\int_{t_0}^t \frac{d}{dt} n_4} \right|^2 + c_2 |g_d - gr(t)|^2 \right\} dt, \quad (19)$$

subject to $(d/dt)n(t) = f(n(t)) + Bs(t) + \text{noise}$, where g_d is the desired growth rate per cycle and x_d the desired composition.

The application of the nonlinear filtering algorithm is demonstrated in Fig. 6 during growth of a parabolic graded 500 Å thick GaInP structure. The PR responses PR75 and PR70 are the feedback signals to control TEG and TMI flows based on nonlinear-filtering techniques and dynamical programming shown in Fig. 5. In this experiment, the filtering output was integrated over ten cycle sequences (60 s, 20 Å resolution) to adjust the control signals for the TEG and TMI flows. The high integration time caused some controller instabilities, observed in the setting of the TMI:TEG flow ratio (see the fluctuations in the flow ratio control signal in Fig. 6), which shows a stepwise adjustment/fluctuation in the TEG and TMI flows. The two insets in Fig. 6 show enlarged the evolutions of the PR signals. (30 s), taken at the same time. The different amplitudes are related to the distinct composition and thickness of the SRL as described by the ROSK model.

Figure 7 shows a off-line analysis and parameter estimation of the PR signals during growth of GaP on Si(001) at 350 °C. The experimental PR signals were recorded for two

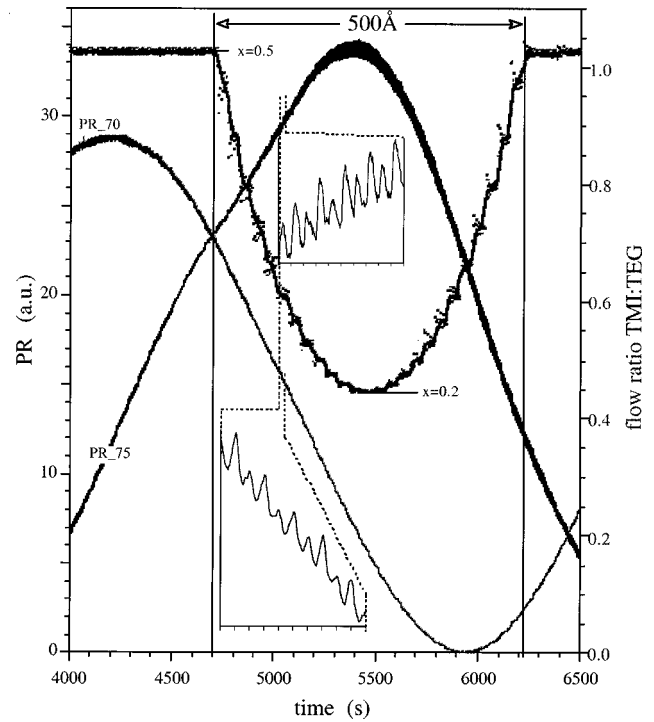


FIG. 6. Closed-loop feedback controlled growth of a 500 Å parabolic Ga_{1-x}In_xP heterostructure.

angles of incidence, $\varphi = 71^\circ$ and $\varphi = 75.2^\circ$, at $\lambda = 650 \pm 5$ nm and at $\lambda = 632.8$ nm, respectively. The two insets in Fig. 7 show, enlarged, the evolutions of the PR signals at different times during growth of GaP on Si(001) and are compared with the simulation. The off-line-simulated responses using the ROSK model and nonlinear filtering are shown with an offset in order to compare it with the experiment.

The steps of the generation of a set of simulated data are shown in detail in Fig. 8 for the TEG pulse 1.3–1.6 s (and TBP pulse 0.0–0.8 s) data. The three SRL components are the result of the source pulses and the ROSK reaction approximations. From the SRL components, the SRL thickness and dielectric function are found. These values then contribute to the calculated reflectance. The fit of the simulated fine structure to the experimental data are shown in Fig. 8(e).³¹ The parameters found by the minimization resulted in $\epsilon_{\text{film}} = 10.6 - 0.06i$; $\epsilon_{\text{Substrate}} = 15.82 - 0.27i$; an average SRL dielectric function of $16.82 - 4.4i$; and an average film growth rate of 0.365 Å/s.

A change in cycle sequence, flow ratio, flux, temperature, or total system pressure, leads to different results, with no predictable correlation found yet. Presently, most of the relevant reactions pathways and their rate constants are not known, with almost no information on reaction kinetic data at growth temperature. Accessing these data will require real-time infrared PRS to analyze molecular-specific absorption signatures and their correlation with real-time mass spectroscopic signals. Such an analysis would allow us to gain a better understanding of the surface reaction kinetics, the validation of the ROSK model, and would provide quan-

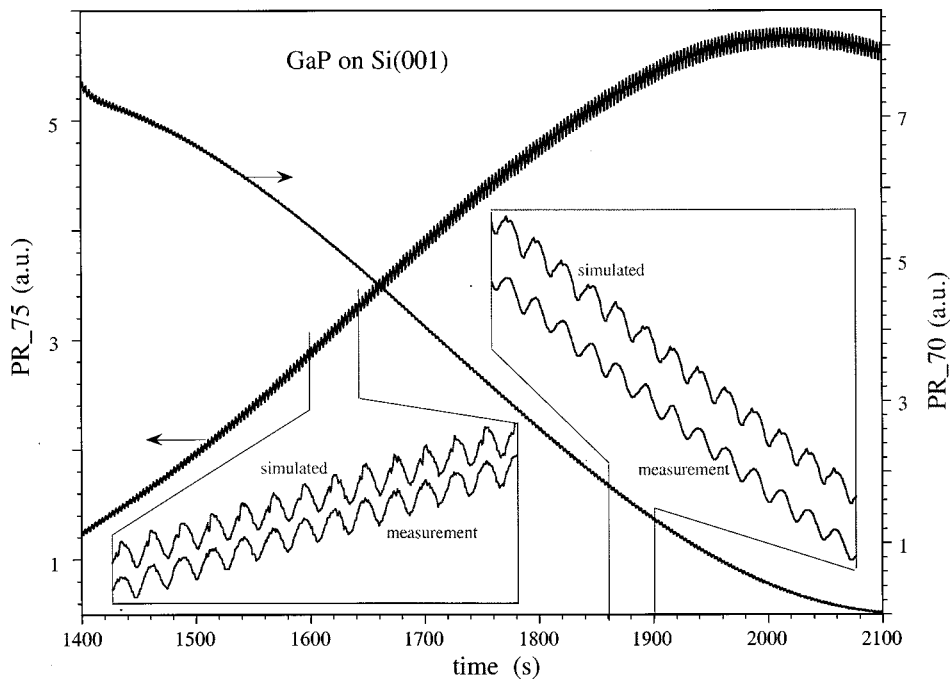


Fig. 7. On-line state estimation of surface kinetics based on two PRS signals.

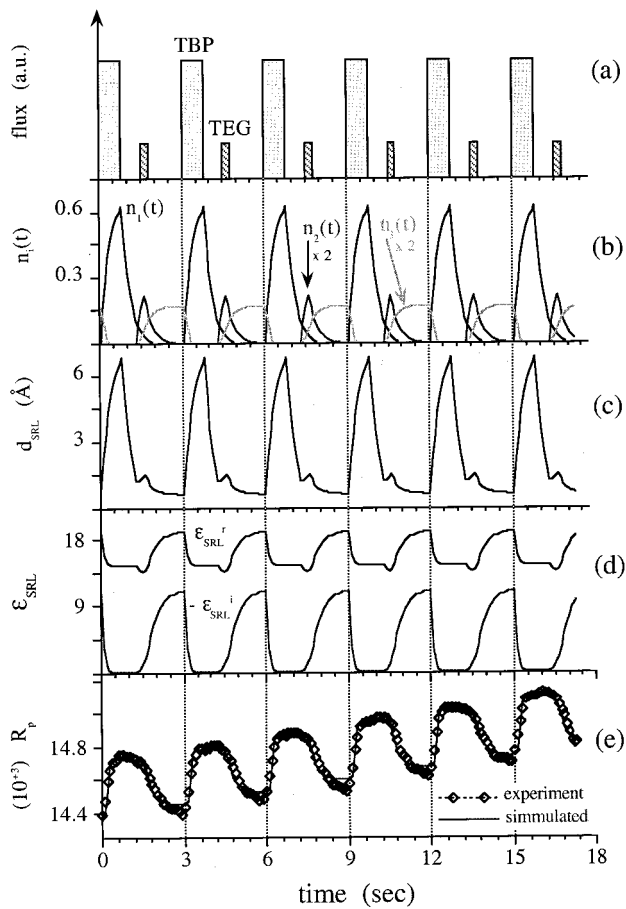


Fig. 8. Simulation of surface reaction kinetics and PR response during heteroepitaxial GaP growth on Si under pulsed organometallic precursors exposure of TBP and TEG. The molar concentrations of the surface constituents, their effective surface layer thickness, and the dielectric optical properties are calculated using Eqs. (5)–(15). The simulated PR response is compared with experimental results obtained at $\varphi = 75.1^\circ$, $\lambda = 632.8$ nm.

titative input parameters for more detailed modeling of the growth process.

IV. SUMMARY

We reported the compositionally and thickness controlled growth of GaInP heterostructures, using PRS as the feedback sensor. An on-line parameter estimate of the state functions $\hat{n}(t)$ using the PRS signals is used to analyze the PRS fine structure and to provide the control signals $s(t)$ for TEG and TMI flows. We introduced a reduced order kinetics model using generalized reaction rate parameters to describe the thickness and composition evolution of the SRL. The molar concentrations n_i in the SRL are directly linked to instantaneous growth rate and composition of the underlying film.

ACKNOWLEDGMENT

This work has been supported by DOD-MURI Grant No. F49620-95-1-0447.

¹S. M. Bedair, B. T. McDermott, Y. Ide, N. H. Karam, H. Hashemi, M. A. Tischler, M. Timmons, J. C. L. Tarn, and N. El-Masry, *J. Cryst. Growth* **93**, 182 (1988).

²C. R. Abernathy, *J. Vac. Sci. Technol. A* **11**, 869 (1993); L. Niinistö and M. Leskel, *Thin Solid Films* **225**, 130 (1993).

³M. Yoshimoto, T. Hashimoto, P. Vaccaro, and H. Matsunami, *Appl. Surf. Sci.* **79-80**, 227 (1994).

⁴D. E. Aspnes, J. P. Harbison, A. A. Studna, and L. T. Florez, *Appl. Phys. Lett.* **52**, 957 (1988).

⁵N. Kobayashi and Y. Horikoshi, *Jpn. J. Appl. Phys., Part 2* **28**, L1880 (1989).

⁶N. Kobayashi and Y. Horikoshi, *Jpn. J. Appl. Phys., Part 2* **29**, L702 (1990).

⁷N. Kobayashi, T. Makimoto, Y. Yamauchi, and Y. Horikoshi, *J. Cryst. Growth* **107**, 62 (1991).

⁸N. Dietz and K. J. Bachmann, *MRS Bull.* **20**, 49 (1995).

⁹N. Dietz and K. J. Bachmann, *Vacuum* **47**, 133 (1996).

- ¹⁰N. Dietz, N. Sukidi, C. Harris, and K. J. Bachmann, *J. Vac. Sci. Technol. A* **15**, 807 (1997).
- ¹¹M. Ebert, K. A. Bell, S. D. Yoo, G. D. Powell, and D. E. Aspnes, *J. Vac. Sci. Technol.* (submitted).
- ¹²D. E. Aspnes, *J. Vac. Sci. Technol. A* **14**, 960 (1996).
- ¹³N. Dietz, A. Miller, and K. J. Bachmann, *J. Vac. Sci. Technol. A* **13**, 153 (1995).
- ¹⁴N. Dietz, A. Miller, J. T. Kelliher, D. Venables, and K. J. Bachmann, *J. Cryst. Growth* **150**, 691 (1995).
- ¹⁵N. Dietz, U. Rossow, D. Aspnes, and K. J. Bachmann, *J. Electron. Mater.* **24**, 1571 (1995).
- ¹⁶K. J. Bachmann, N. Dietz, A. E. Miller, D. Venables, and J. T. Kelliher, *J. Vac. Sci. Technol. A* **13**, 696 (1995).
- ¹⁷K. J. Bachmann, U. Rossow, N. Sukidi, H. Castleberry, and N. Dietz, *J. Vac. Sci. Technol. B* **14**, 3019 (1996).
- ¹⁸N. Dietz, U. Rossow, D. E. Aspnes, and K. J. Bachmann, *Appl. Surf. Sci.* **102**, 47 (1996).
- ¹⁹N. Dietz, N. Sukidi, C. Harris, and K. J. Bachmann, *Mater. Res. Soc. Symp. Proc.* **441**, 39 (1997).
- ²⁰K. J. Bachmann, N. Sukidi, N. Dietz, C. Hoepfner, S. LeSure, H. T. Tran, S. Beeler, K. Ito, and H. T. Banks, *J. Cryst. Growth* **183**, 323 (1998).
- ²¹N. Dietz, N. Sukidi, C. Harris, and K. J. Bachmann, in *Proceedings of the Ninth International Conference on Indium Phosphide and Related Materials (IPRM-9)* 11–15 May 1997, p. 521.
- ²²K. J. Bachmann, C. Hoepfner, N. Sukidi, A. E. Miller, C. Harris, D. E. Aspnes, N. Dietz, H. T. Tran, S. Beeler, K. Ito, H. T. Banks, and U. Rossow, *Appl. Surf. Sci.* **112**, 38 (1997).
- ²³N. Dietz and K. Ito, *Thin Solid Films* **313-314**, 615 (1998).
- ²⁴J. T. Kelliher, N. Dietz, and K. J. Bachmann, in *The Kinetics of Chemical Beam Epitaxy of Gallium Phosphide*, Proceedings of SOTAPOCS 18, Honolulu, Hawaii (The Electrochemical Society, Pennington, NJ, 1994), p. 17.
- ²⁵A. J. Murrell, A. T. S. Wee, D. H. Fairbrother, N. K. Singh, J. S. Foord, G. J. Davies, and D. A. Andrews, *J. Cryst. Growth* **105**, 199 (1990).
- ²⁶K. J. Bachmann, U. Rossow, and N. Dietz, *Mater. Sci. Eng., B* **37**, 472 (1995).
- ²⁷D. E. Aspnes, *J. Opt. Soc. Am. A* **10**, 974 (1993).
- ²⁸D. E. Aspnes, *Appl. Phys. Lett.* **62**, 343 (1993).
- ²⁹D. E. Aspnes, U.S. Patent No. 5,277,747, issued 11 January 1994.
- ³⁰K. Ito and K. Xiong, *IEEE Trans. Autom. Control* (to be published).
- ³¹S. Beeler, H. T. Tran, and N. Dietz, *J. Appl. Phys.* (submitted).